Supplementary Material

Text S1. Seagrass Ecosystem Conditions

Throughout the summer, Zostera blade length increased and was the dominant microorganisms. For example, *Zostera* blades had an average length of 28.1 cm in June, increasing to an average of 52.7 cm by September. *Polysiphonia* and *Zostera* biomass per square meter peaked in July (34 and 57 g m^{-2}, respectively) with lower density in June (20 and 41 g m^{-2}, respectively) and September (2 and 41 g m^{-2}, respectively). Epiphytes increased slowly to a peak in September (~30 g m^{-2}), when they had higher biomass density than *Polysiphonia*

Seagrass density was quantified by counting all shoots within six 0.0625 m^2 quadrants randomly located within 50 meters of the seagrass incubation site. The length and widths of each seagrass shoot was measured followed by the removal and collection of epiphyte biomass (if present). The seagrass, epiphytes, and algae biomass were quantified by mass after being dried in an oven at 60˚C for 2 to 5 days, or until the biomass no longer decreased in weight. Temperature and dissolved oxygen concentrations were also measured continuously throughout the entire summer using a factory-calibrated Rinko III (JFE Advantech) (Coogan and Long, 2023).

The environmental conditions that correspond with the incubations (PAR, temperature, salinity, dissolved oxygen, and pH) were measured hourly throughout the incubations and were averaged (± standard deviations) across the incubation timeframe (~0900 to ~1400) (**Table S1**). PAR varied depending on cloud coverage, with average PAR across all sample days ranging from 545 ± 262 to 3260 ± 807 µmol photons m^{-2} s^{-1}. Temperature varied less between sample days, ranging from an average of 20.2 ± 1.0 to 24.5 ± 0.5 ˚C, with June being the coolest and July being the warmest month. Salinity at the site was greater in June (30.0 ± 2.4 to 34.0 ± 0.9 practical salinity units, PSU) than July and September (21.7 ± 1.8 to 23.3 ± 0.4 PSU), which could be due to temporal and tidal influences from the adjacent marsh. Dissolved oxygen concentrations co-varied with PAR, with the percent saturation averaging between 117.6 ± 18.9 and 197.0 ± 18.7 % during the day and 108.2 ± 5.8 % during the evening. The pH (measured on NBS scale) was similar across all sample days, ranging between 8.0 ± 0.2 and 8.5 ± 0.6, and did not correlate with any other environmental measurements ($R^2 < 0.294$ for pH vs. PAR, O_2, temperature, and salinity).

Text S2. Oxygen dynamics within seagrass ecosystem

Oxygen concentration measurements were completed using a FireSting GO_2 field oxygen meter (PyroScience GmbH). Which was calibrated with air prior to each use. O_2 concentrations were automatically temperature compensated with an integrated temperature sensor (temperature averaged 22.5 ± 0.7˚C). The specific fluxes of Polysiphonia and Zostera were seawater corrected and biomass normalized. Briefly, for all incubations the oxygen flux was calculated by taking the slope of oxygen concentrations for all replicates across the sampling period. To correct for the seawater contribution, oxygen fluxes for *Polysiphonia* and *Zostera* (µmol hr^{-1}) were determined by subtracting the observed oxygen fluxes in the seawater control incubations from those of the photosynthetic macrophyte incubations which contained the same volume of seawater. These fluxes were then normalized to biomass dry weight, as described above (µmol g dry wt^{-1} hr^{-1}). The seawater control was normalized by volume (µmol L^{-1} hr^{-1}). The daytime (~0900 to ~1400)

incubations were used to calculate net oxygen fluxes and were scaled up to the ~15 hours of daylight for June and July and ~13 hours for September. The evening (~1900 to ~2300) incubations were used to calculate respiration (R) and were scaled up to the 24 hours a day that respiration was occurring. For the areal NPP flux calculations, within seawater control incubations, the flux (µmol L^{-1} hr^{-1}) was multiplied by the average water depth of the seagrass ecosystem (2 meters). All rates were then adjusted to daily rates by accounting for the number of hours that the fluxes were occurring during the day (15 h for June and July, 13 h for September per day) and respiration during the day and night (24 hours per day).

Relative to the variable areal oxygen NPP in the seawater (ranging from -94 to 74 mmol O_2 m^{-2} d^{-1}), *Polysiphonia* contributed minimally to the areal oxygen NPP (average per season ranging from 1.3 to 1.9 mmol O_2 m^{-2} d^{-1}), while the *Zostera* contributed to areal NPP at a rate (average per season ranging from 31.3 to 58.2 mmol O_2 m^{-2} d^{-1}) exceeding most net ecosystem metabolism (NEM) rates presented by previous studies (**Figure 4**). Although direct comparisons with previous studies are challenging due to methodological differences (i.e. ecosystem scale vs. individual species, techniques such as laboratory incubations, benthic chambers, oxygen mass balances, etc.), reported NEM rates across an array of seagrass ecosystems spanning temperate regions range from -107 to 38 mmol O_2 m^{-2} d^{-1} (Duarte et al., 2010; Long et al., 2015; Long et al., 2019). Previous studies have shown that processes occurring in above ground biomass were not necessarily correlated with rhizome processes below ground (Alexandre *et al.*, 2011; Van Engeland *et al.*, 2011). Given that this study only incubated the above ground biomass of *Zostera* and did not consider all ecosystem processes (i.e. micro- and macro-algae, sediments, organisms, etc), it may not be surprising that rates of O_2 produced by *Zostera* and those from the seawater extend to higher ranges within this study than previously observed for the entire ecosystem. Uniquely, this study isolated the oxygen flux and NPP associated with background seawater from specific organisms (*Polysiphonia* and *Zostera*) to understand their specific contribution to oxygen production within the larger ecosystem. This is different from most previous studies, which measured the combined fluxes of seawater, photosynthetic macrophytes, and other non-specified ecosystem influences (Berger et al., 2020; Duarte et al., 2010; Long et al., 2019). Isolation of the species-specific oxygen fluxes highlights *Polysiphonia* as a smaller source of oxygen flux (monthly average ~3 to 78 µmol O_2 g dry wt^{-1} h^{-1}) and NPP (monthly average ~13 to 88 µmol O_2 g dry wt^{-1} h^{-1}) compared to *Zostera* oxygen fluxes (monthly average ~40 to 108 µmol O_2 g dry wt^{-1} h^{-1}) and NPP (monthly average ~70 to 137 µmol O_2 g dry wt^{-1} h^{-1}). Given the nuances that this study highlights in oxygen fluxes and NPP rates produced by the seawater and photosynthetic macrophytes, additional investigations are required to focus on species specific influences within the ecosystem to understand the roles they currently play in oxygen fluxes and how these fluxes could evolve as ecosystem compositions may shift under changing climates.

All incubations with *Polysiphonia* and *Zostera* exhibited net photosynthesis during the day that exceeded the daily rates of respiration, suggesting that the observed components were likely contributing to net autotrophy and hence, could play a role in carbon sequestration (***Figure 2 and 3***). Ecosystems that are net autotrophic have daily NPP rates greater than daily respiration rates (R) (NPP:R >1), which also indicates the flow of carbon in the system, where autotrophic ecosystems contribute to carbon uptake by fixing more carbon than they release (Duarte *et al.*, 2010; Berger *et al.*, 2020). Globally, seagrass ecosystems have generally been shown to be net autotrophic (Murray and Wetzel, 1987; Duarte *et al.*, 2010; Long *et al.*, 2019), with an NPP:R

averaging 1.55 ± 0.13 across 155 different seagrass sites (Duarte *et al.*, 2010). Within the seawater control, NPP:R was near 1 – specifically, slightly below 1 during June (0.93 ± 0.02) and slightly above 1 in July and September (1.05 ± 0.03 and 1.04 ± 0.02, respectively). This demonstrates the relatively minor contribution of the components within the seawater control incubation (i.e. microbes, phytoplankton, small zooplankton, etc) to the overall net ecosystem metabolism, with its slight influence shifting from heterotrophy in the beginning of the summer to autotrophy towards the end. On the other hand, *Polysiphonia* and *Zostera* are large contributors to autotrophy in this ecosystem, with NPP:R for both species lowest in July (1.25 ± 0.35 and 2.33 ± 1.28, respectively) and highest in September (8.70 ± 3.11 and 4.60 ± 2.44, respectively). By isolating species-specific metabolic rates of both *Polysiphonia*, and *Zostera*, this study clearly highlights the major contribution of these photosynthetic organisms as drivers of autotrophy in these ecosystems.

Given our derived oxygen NPP values and assuming the photosynthetic quotient of 1 mole O_2 : 1 mole CO_2 (Duarte *et al.*, 2010), the monthly average oxygen production within *Zostera* incubations corresponds with a carbon uptake rate ranging from 74 to 255 g C m^{-2} yr^{-1}, with *Polysiphonia* contributing much less (6 to 8 g C m^{-2} yr^{-1}). It is estimated that seagrass ecosystems cover ~300,000 to 600,000 km^2 (Fourqurean *et al.*, 2012), and therefore the carbon uptake rate by *Zostera* alone could correspond to global carbon uptake of ~72 Tg C yr^{-1}. This carbon uptake potential by *Zostera* alone is within the upper range of carbon storage potential calculated from other seagrass ecosystems (between ~20 to ~100 Tg C $year^{-1}$ globally; Novak et al., 2020; Röhr et al., 2018), including Cape Cod (8 to 230 g C m^{-2} yr^{-1}, which corresponds to ~4 to ~104 Tg C yr^{-1}; Novak et al., 2020). It is expected that our study reports carbon storage estimates at the higher end of the range since only the aboveground seagrass was measured (excluding respiration rates in the sediments), and rates were only measured during the summer months (excluding lower productivity during the winter). Similarly, other studies suggest that these techniques to estimate seagrass carbon storage may either be an overestimation due to the lack of consideration of bioturbation and carbon remineralization within sediments (Johannessen and Macdonald, 2016), or an underestimation, if comparing to studies that measured high sedimentation rates that trap organic carbon and dead rhizomes (Röhr *et al.*, 2018; Novak *et al.*, 2020). The results from this study nonetheless underscore the need to further assess the role that seagrass ecosystems play as potential regions of blue carbon storage (Pendleton *et al.*, 2012; Duarte *et al.*, 2013; Kuwae and Hori, 2019).

Text S3. Hydrogen peroxide POHPPA method and decay rate constants

Hydrogen peroxide concentration was measured using the POHPPA (4-hydroxyphenylacetic acid) technique and associated protocols (Miller *et al.*, 2005; Shaked and Armoza-Zvuloni, 2013; Sutherland *et al.*, 2021). Briefly, the reaction between POHPPA reagent and hydrogen peroxide was catalyzed by horseradish peroxidase to form a fluorescent dimer. The POHPPA reagent was prepared with 0.25mM POHPPA, 70 units mL^{-1} of horseradish peroxidase, and 0.25M Tris buffer (pH 8.8). Aliquots of samples (5 mL) were mixed with reagent promptly after collection in a 1:50 reagent:sample ratio and incubated in amber glass vials. Fluorescence was measured using a Molecular Devices SpectraMax M3 with excitation 315 nm and emission

408 nm. Tests indicated that after the addition of POHPPA, sample signal was stable for up to 10 hours. All samples here were analyzed within 4 hours of collection.

Hydrogen peroxide standards were prepared at the time of sample collection by filtering the sample water via syringe filter (0.22 μm membrane filter) and amending it with hydrogen peroxide (3% H_2O_2 w/w, Sigma) prior to the POHPPA reagent. Hydrogen peroxide stock solutions were quantified each day by molar absorptivity (240 nm) measured using a UV spectrophotometer, which ranged between 0.485 and 0.487. The blank was prepared by amending filtered incubation water with catalase (25 units mL^{-1}, Sigma) prior to the addition of POHPPA reagent. The fluorescence of standards and blanks were measured alongside the samples as described above.

Using the POHPPA method, hydrogen peroxide decay rate constants were quantified in duplicate by amending 20 mL of incubation water collected from seawater control incubations, *Polysiphonia,* and *Zostera* at the second time point with 1 μM H_2O_2 in dark, glass vials. Hydrogen peroxide concentrations were measured at 0, 0.5, 1, and 2 hours by taking a 1 mL aliquot. Decay rate constants were calculated using a pseudo-first order decay, as observed previously for hydrogen peroxide decay (Shaked and Armoza-Zvuloni, 2013). These POHPPA decay rate constants measure the decay of the filtered water during a dark incubation. By comparison, the isotope method captured decay deriving from *in situ* incubation conditions with and without the presences of *Polysiphonia* and *Zostera*.

Specifically, $k_{loss,POHPPA}$ (only measured in July and September) ranged from 0.140 h^{-1} (July) to 0.205 h^{-1} (September) for seawater control incubations. *Polysiphonia* and *Zostera* incubations had faster decay rate constants than the seawater control and $k_{loss,POHPPA}$ was similar across July and September for both *Polysiphonia* (0.723 and 0.668 h^{-1}, respectively) and *Zostera* (0.427 and 0.384 h^{-1}, respectively). As a reminder, the POHPPA method measured decay of filtrate from the incubations under dark conditions, whereas the isotope method measured decay directly occurring in the *in situ* incubations. Therefore, the $k_{loss,isotope}$ is used for all further calculations and discussion since it better reflects reactions occurring under *in situ* conditions.

Text S4. Sample preparation and reporting for isotope ratio mass spectrometry

At the time of analysis, a gas-tight syringe filled with 50μl of UHP He (99.999%) was expelled while inserting into the 2 mL serum sample vial. The gas volume withdrawn from the sample vial was always less than the volume of He added, thus ensuring that the sample vials were over pressurized relative to the ambient laboratory atmospheric pressure. The sample gas and He carrier gas mixture were withdrawn from the sample vial and an additional 50 μL was expelled from the gas-tight syringe prior to introduction to the isotope ratio mass spectrometer (IRMS) via injection port (Sutherland *et al.*, 2021). This approach reduced the possibility of atmospheric gas entering and contaminating either the sample vial or gas-tight syringe.

Using a helium carrier flow, sample N_2, O_2 and Ar were dried by passing through two Nafion dryers (Permapure, Inc.) linked in series, chromatographically separated using a packed 2 m Molsieve 5*Å* gas chromatography column (1/16" OD; Restek 19001), and then routed to an IsoPrime 100 isotope ratio mass spectrometer. This IsoPrime 100 has Faraday cups for each mass to charge (m/z) ratio, allowing for simultaneous quantification of nitrogen (m/z: 28, 29, 30),

oxygen (m/z: 32, 33, 34), and argon (m/z: 40) without requiring peak jumping. Analysis of each sample is reported relative to pairwise measurements of reference gas before and after sample measurement. Ion beam intensities were integrated and normalized against the major beam for each species (m/z 28 for nitrogen, and m/z 32 for oxygen). The O_2:N_2 (m/z = 32/28) ratio was measured to verify the isotopic composition of the sample and used to quality control data and identify contamination. The O_2:Ar (m/z = 32/40) ratio was also measured and used to interpret biological activity within the samples. Finally, each analytical session also included multiple analyses (across a range of sizes) of well-mixed laboratory air (23.1 ± 1.7 ºC) as a standard using the same IRMS preparatory system as above.

The mass spectrometric analysis in this study tracked the evolution of the ^{17}O-^{17}O isotopologue (m/z 34) into the dissolved O_2 reservoir, and samples were therefore analyzed in the same way that conventional oxygen-18 analyses are conducted (^{16}O-^{18}O, also m/z 34). Accordingly, all isotope data produced in this study were recorded as the $\delta^{18}O$ equivalent ($\delta^{18}O = (^{18}R_{sample}/^{18}R_{standard} - 1)*1000$, $R = ^{18}O/^{16}O$). These values were then converted to ^{34}R ($^{34}R = ^{34}O_2/^{32}O_2$) and used for calculations as described below. The volumes of the injected laboratory air standards were 30 µL, 50 µL, and 70 µL, and at 23.1ºC correspond to 2.6 x 10^{-7}, 4.3 x 10^{-7}, and 6.0 x 10^{-7} moles of O_2 respectively via ideal gas law equation of state. The injection standard error across all three standard sizes was 4.4 x 10^{-10} moles for ^{16}O-^{17}O, and 4.5 x 10^{-10} moles for ^{17}O-^{17}O. Delta values for the laboratory standards and samples are reported against the accepted isotopic composition of air having $\delta^{18}O$ of 24.046 ‰ against the VSMOW2 standard (Wostbrock *et al.*, 2020). Typical analytical uncertainty for $\delta^{18}O$ is ±0.20 ‰ (standard deviation of replicate standard analyses).

Supplemental Figures and Tables

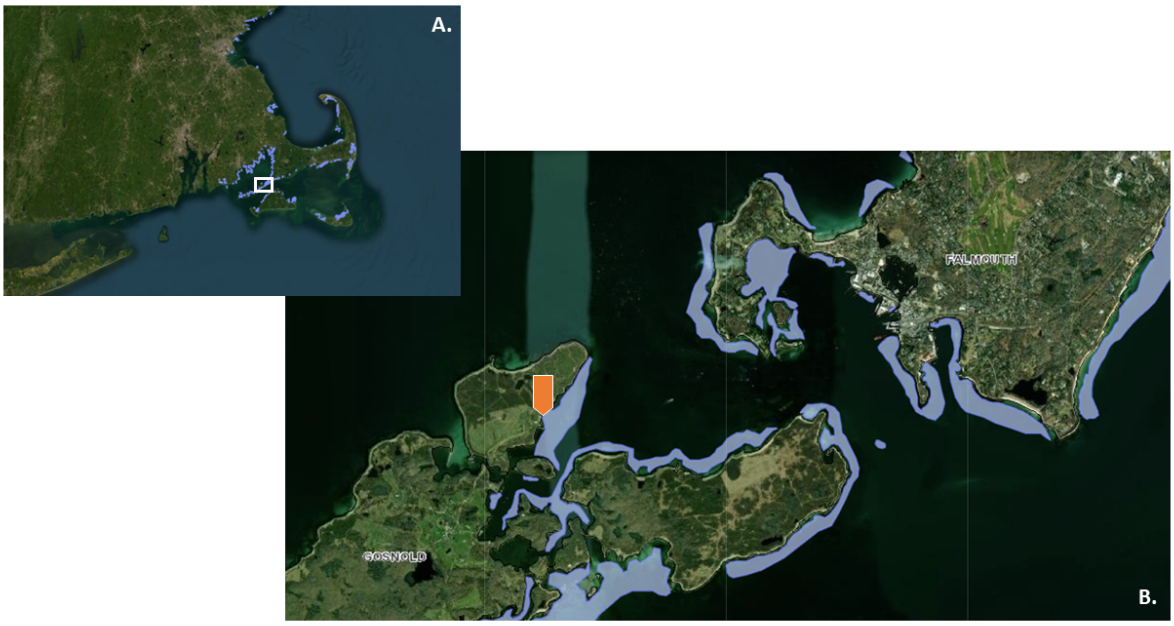

Figure S1. Map of seagrass ecosystem (MassGIS) with A.) showing the large-scale map of the seagrass located off the southwest end of Woods Hole and B.) showing the smaller-scale version of the seagrass ecosystem. The sample site is marked by an orange arrow and seagrass ecosystems are outlined in blue. Maps were created by Earthstar Geographics Massachusetts Department of Environmental Protection. Blue areas highlight the Eel Grass Mapping Project from MassGIS.

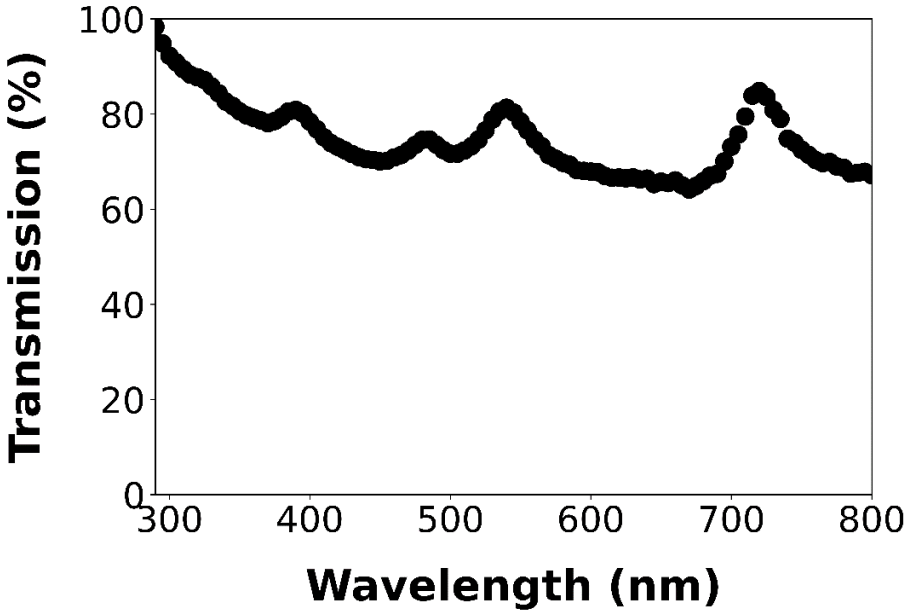

Figure S2. Percent transmission of light through Tedlar bagacross wavelengths ~200-800nm. Tedlar transmits 64 to 84% of the sunlight, which does not vary significantly for wavelengths between 400-800nm. This percentage is within the range of natural variation across sampling days, which ranges between 10 to 80% (average 60%) less sunlight than the sunniest day, likely due to cloud cover.

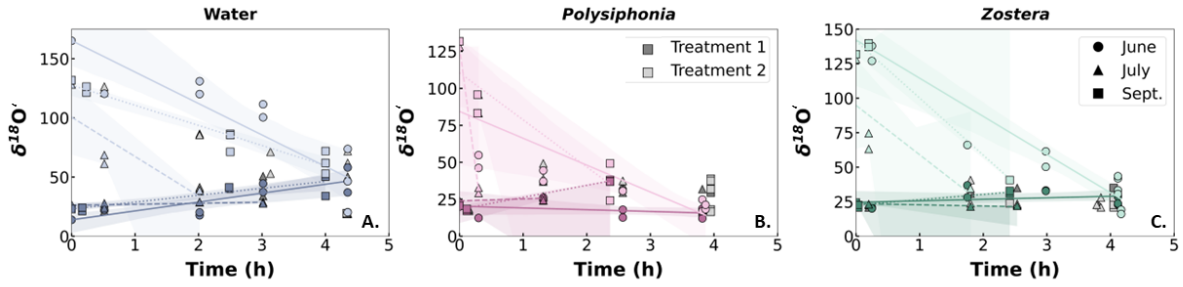

Figure S3. Oxygen isotope signature ($\delta^{18}O'$, y-axis) across time (h, x-axis) for incubations in A.) water (blue), B.) *Polysiphonia* (pink), and C.) *Zostera* (green). The bottom (dark shade) data on each graph represent Treatment 1 (no additions, O_2 only) and the top (light shade) data on each graph represent Treatment 2 (added permanganate, O_2 + H_2O_2). Individual data points are presented, and the colored data points are used to create a line of best fit (shaded region represents 95% confidence interval, solid line is June, dashed is July, dotted is September) and calculate k_{loss}. The gray points are not used in any calculations because they are after the initial decay of hydrogen peroxide.

Table S1. Environmental parameters of the ambient seawater near the incubations during the concentration and decay pathway sampling days (June, July, and September) and night (September) for each sampling period. Average and standard deviation is reported for the measurements across time points that were taken each hour during the entirety of the incubations. Displayed is the photosynthetically active radiation (PAR, µmol m^{-2} s^{-1}), temperature (temp, ˚C), salinity (practical salinity units, PSU), dissolved oxygen (% Saturation), and pH.

Date	Time of Day	Incubation Type	Measurement	PAR (µmol m^{-2} s^{-1})	Temperature (°C)	Salinity (PSU)	Dissolved Oxygen (% Saturation)	pH
7-Jun-21	Day	Concentration	avg	1046.0	20.2	30.0	154.0	8.4
			std dev	58.5	1.0	2.4	4.9	0.1
9-Jun-21	Day	Decay	avg	3258.2	22.0	34.0	134.6	8.3
			std dev	807.1	1.9	0.9	10.9	0.3
20-Jul-21	Day	Concentration	avg	2878.1	24.6	23.3	197.0	8.5
			std dev	450.7	0.5	0.4	18.7	0.6
14-Jul-21	Day	Decay	avg	545.0	21.7	22.9	117.6	8.0
			std dev	262.3	0.7	0.4	18.9	0.2
16-Jul-21	Day	Decay	avg	1162.5	23.2	23.2	152.4	8.1
			std dev	102.5	0.4	0.7	21.2	0.3
3-Sep-21	Day	Concentration	avg	1021.9	23.3	22.9	144.1	8.3
			std dev	125.3	0.7	0.3	20.8	0.1
3-Sep-21	Night	Concentration	avg	NA	22.9	22.9	108.2	8.3
			std dev	NA	0.2	0.0	5.8	0.0
13-Sep-21	Day	Decay	avg	886.4	22.5	21.7	145.2	8.2
			std dev	219.1	0.4	1.8	14.4	0.1

Table S2. Average and standard deviation values of O2 and H2O2 flux, net production and areal net production for water, *Polysiphonia*, and *Zostera* incubations across each month for day (all months) and night (only September). Units for each measurement are displayed. The fluxes measured in liters (i.e. L^{-1}) correspond to the water incubations and the fluxes measured in grams of dry weight (i.e. g^{-1}) correspond to the *Polysiphonia* and *Zostera* incubations.

Species	Month	Time of Day	O_2 Flux		O_2 Net Production		O_2 Areal NPP		H_2O_2 Flux		H_2O_2 Net Production		H_2O_2 Areal Net Production	
			μmol L^{-1} hr^{-1} or μmol g^{-1} hr^{-1}		μmol L^{-1} hr^{-1} or μmol g^{-1} hr^{-1}		mmol day^{-1} m^{-2}		nmol L^{-1} hr^{-1} or nmol g^{-1} hr^{-1}		nmol L^{-1} hr^{-1} or nmol g^{-1} hr^{-1}		mmol day^{-1} m^{-2}	
			Average	Std Dev	Average	Std Dev	Average	Std Dev	Average	Std Dev	Average	Std Dev	Average	Std Dev
Water	June	Day	**-3.2**	1.1	**44.3**	1.1	**-93.9**	33.1	**282.4**	63.8	**2017.4**	187.6	**60.5**	5.6
Polysiphonia	June	Day	**4.8**	2.4	**14.9**	2.4	**1.5**	0.7	**-213.0**	91.2	**216.3**	453.0	**0.1**	0.1
Zostera	June	Day	**50.9**	33.6	**80.7**	33.6	**31.3**	20.7	**149.9**	612.2	**1496.0**	4619.9	**0.9**	2.8
Water	July	Day	**2.4**	1.4	**49.9**	1.4	**74.0**	42.6	**130.5**	19.8	**2001.8**	158.5	**60.1**	4.8
Polysiphonia	July	Day	**2.5**	3.6	**14.4**	3.1	**1.3**	1.8	**132.3**	101.1	**38033.3**	10451.1	**9.8**	2.7
Zostera	July	Day	**39.7**	38.1	**69.5**	38.1	**34.2**	32.8	**-115.0**	77.8	**4863.6**	2453.2	**4.2**	2.1
Water	September	Day	**2.3**	0.8	**49.7**	0.8	**61.5**	20.7	**187.5**	70.5	**2510.2**	618.0	**65.3**	16.1
Polysiphonia	September	Day	**77.7**	31.4	**87.8**	31.4	**1.9**	0.8	**-271.7**	269.0	**-2212.2**	4625.2	**0.0**	0.1
Zostera	September	Day	**107.5**	72.8	**137.4**	72.8	**58.2**	39.4	**106.6**	172.0	**19103.0**	22660.2	**10.3**	12.3
Water	September	Night	**-47.5**	0.5					**-104.3**	28.4				
Polysiphonia	September	Night	**-10.1**	2.2					**62.8**	214.7				
Zostera	September	Night	**-29.9**	9.4					**-722.9**	576.8				

Table S3. The top table displays one-way ANOVA values for oxygen and hydrogen peroxide fluxes within seawater control, background corrected *Polysiphonia*, and background corrected *Zostera* incubations across sample periods. The bottom table displays T-test p-values for background corrected *Polysiphonia* and background corrected *Zostera* incubations to indicate which incubations are significantly different than the seawater control. All statistical tests were completed between all seasons and each sample period compared against one another for each incubation condition. The "*" indicates that the difference between the categories tests was significant (ANOVA and T-test p-value < 0.05).

Sampling Campaign Comparisons (ANOVA p-values)					
		All Seasons	**June-July**	**July-Sept**	**Sept-June**
Oxygen Fluxes	**Seawater control**	0.000*	0.002*	0.909	0.000*
	Polysiphonia	0.006*	0.490	0.017*	0.019*
	Zostera	0.095	0.615	0.085	0.109
H_2O_2 Fluxes	**Seawater control**	0.026*	0.008*	0.226	0.135
	Polysiphonia	0.079	0.010*	0.091	0.733
	Zostera	0.696	0.309	0.014*	0.869

Seawater Control Comparison (t-test)					
		All Seasons	**June**	**July**	**Sept**
Oxygen Fluxes	***Polysiphonia***	0.018*	0.036*	0.174	0.008*
	Zostera	0.000*	0.004*	0.026*	0.004*
H_2O_2 Fluxes	***Polysiphonia***	0.043*	0.009*	0.076	0.068
	Zostera	0.279	0.255	0.004*	0.076

Table S4. Regression coefficients (R^2) and T-test p-values for comparison between oxygen fluxes and hydrogen peroxide fluxes (Fluxes) and oxygen net primary production (NPP) and net hydrogen peroxide production (Net Production). Values are reported for seawater control, background corrected *Polysiphonia*, and background corrected *Zostera* incubations. The "*" indicates that the difference between the categories tested was significant (T-test p-values > 0.05 and R^2 > 0.63).

Incubation	Month	Fluxes		Net Production	
		R^2	T-test P-Value	R^2	T-test P-Value
Seawater Control	June	0.128	0.618	0.133	0.598
	July	0.090	0.594	0.014	0.859
	September	0.164	0.556	0.266	0.416
Polysiphonia	June	0.839*	0.056	0.021	0.893
	July	0.828*	0.061	0.828*	0.037*
	September	0.761*	0.017*	0.513	0.173
Zostera	June	0.169	0.838	0.117	0.426
	July	0.610	0.002*	0.670*	0.019*
	September	0.279	0.787	0.701*	0.007*

LITERATURE CITED

Alexandre, A., Silva, J., Bouma, T.J. and Santos, R. (2011) 'Inorganic nitrogen uptake kinetics and whole-plant nitrogen budget in the seagrass Zostera noltii', *Journal of Experimental Marine Biology and Ecology*, 401(1–2), pp. 7–12. doi:10.1016/j.jembe.2011.03.008.

Berger, A.C., Berg, P., McGlathery, K.J. and Delgard, M.L. (2020) 'Long-term trends and resilience of seagrass metabolism: A decadal aquatic eddy covariance study', *Limnology and Oceanography*, 65(7), pp. 1423–1438. doi:10.1002/lno.11397.

Coogan, J. and Long, M.H. (2023) 'Development and deployment of a long-term aquatic eddy covariance system', *Limnology and Oceanography: Methods*, p. lom3.10564. doi:10.1002/lom3.10564.

Duarte, C.M., Kennedy, H., Marbà, N. and Hendriks, I. (2013) 'Assessing the capacity of seagrass meadows for carbon burial: Current limitations and future strategies', *Ocean & Coastal Management*, 83, pp. 32–38. doi:10.1016/j.ocecoaman.2011.09.001.

Duarte, C.M., Marbà, N., Gacia, E., Fourqurean, J.W., Beggins, J., Barrón, C. and Apostolaki, E.T. (2010) 'Seagrass community metabolism: Assessing the carbon sink capacity of seagrass meadows', *Global Biogeochemical Cycles*, 24(4). doi:https://doi.org/10.1029/2010GB003793.

Fourqurean, J.W., Duarte, C.M., Kennedy, H., Marbà, N., Holmer, M., Mateo, M.A., Apostolaki, E.T., Kendrick, G.A., Krause-Jensen, D., McGlathery, K.J. and Serrano, O. (2012) 'Seagrass ecosystems as a globally significant carbon stock', *Nature Geoscience*, 5(7), pp. 505–509. doi:10.1038/ngeo1477.

Johannessen, S.C. and Macdonald, R.W. (2016) 'Geoengineering with seagrasses: is credit due where credit is given?', *Environmental Research Letters*, 11(11), p. 113001. doi:10.1088/1748-9326/11/11/113001.

Kuwae, T. and Hori, M. (eds) (2019) *Blue Carbon in Shallow Coastal Ecosystems: Carbon Dynamics, Policy, and Implementation*. Singapore: Springer Singapore. doi:10.1007/978-981-13-1295-3.

Long, M., Berg, P., McGlathery, K. and Zieman, J. (2015) 'Sub-tropical seagrass ecosystem metabolism measured by eddy covariance', *Marine Ecology Progress Series*, 529, pp. 75–90. doi:10.3354/meps11314.

Long, M.H., Rheuban, J.E., McCorkle, D.C., Burdige, D.J. and Zimmerman, R.C. (2019) 'Closing the oxygen mass balance in shallow coastal ecosystems', *Limnology and Oceanography*, 64(6), pp. 2694–2708. doi:10.1002/lno.11248.

Miller, G.W., Morgan, C.A., Kieber, D.J., King, D.W., Snow, J.A., Heikes, B.G., Mopper, K. and Kiddle, J.J. (2005) 'Hydrogen peroxide method intercomparision study in seawater', *Marine Chemistry*, 97(1–2), pp. 4–13. doi:10.1016/j.marchem.2005.07.001.

Murray, L. and Wetzel, R. (1987) 'Oxygen production and consumption associated with the major autotrophic components in two temperate seagrass communities', *Marine Ecology Progress Series*, 38, pp. 231–239. doi:10.3354/meps038231.

Novak, A.B., Pelletier, M.C., Colarusso, P., Simpson, J., Gutierrez, M.N., Arias-Ortiz, A., Charpentier, M., Masque, P. and Vella, P. (2020) 'Factors Influencing Carbon Stocks and Accumulation Rates in Eelgrass Meadows Across New England, USA', *Estuaries and Coasts*, 43(8), pp. 2076–2091. doi:10.1007/s12237-020-00754-9.

Pendleton, L., Donato, D.C., Murray, B.C., Crooks, S., Jenkins, W.A., Sifleet, S., Craft, C., Fourqurean, J.W., Kauffman, J.B., Marbà, N., Megonigal, P., Pidgeon, E., Herr, D., Gordon, D. and Baldera, A. (2012) 'Estimating Global "Blue Carbon" Emissions from Conversion and Degradation of Vegetated Coastal Ecosystems', *PLoS ONE*. Edited by S. Thrush, 7(9), p. e43542. doi:10.1371/journal.pone.0043542.

Röhr, M.E. et al. (2018) 'Blue Carbon Storage Capacity of Temperate Eelgrass (*Zostera marina*) Meadows', *Global Biogeochemical Cycles*, 32(10), pp. 1457–1475. doi:10.1029/2018GB005941.

Shaked, Y. and Armoza-Zvuloni, R. (2013) 'Dynamics of hydrogen peroxide in a coral reef: Sources and sinks: H_2O_2 dynamics in a coral reef', *Journal of Geophysical Research: Biogeosciences*, 118(4), pp. 1793–1801. doi:10.1002/2013JG002483.

Sutherland, K.M., Grabb, K.C., Karolewski, J.S., Taenzer, L., Hansel, C.M. and Wankel, S.D. (2021) 'The redox fate of hydrogen peroxide in the marine water column', *Limnology and Oceanography*, 66(10), pp. 3828–3841. doi:10.1002/lno.11922.

Van Engeland, T., Bouma, T., Morris, E., Brun, F., Peralta, G., Lara, M., Hendriks, I., Soetaert, K. and Middelburg, J. (2011) 'Potential uptake of dissolved organic matter by seagrasses and macroalgae', *Marine Ecology Progress Series*, 427, pp. 71–81. doi:10.3354/meps09054.

Wostbrock, J.A.G., Cano, E.J. and Sharp, Z.D. (2020) 'An internally consistent triple oxygen isotope calibration of standards for silicates, carbonates and air relative to VSMOW2 and SLAP2', *Chemical Geology*, 533, p. 119432. doi:10.1016/j.chemgeo.2019.119432.